OES Faculty Publications   Ocean & Earth Sciences

2023

The Vulnerability and Resilience of Seagrass Ecosystems to Marine Heatwaves in New Zealand: A Remote Sensing Analysis of Seascape Metrics Using PlanetScope Imagery

Ken Joseph E. Clemente
University of Canterbury

Mads S. Thomsen
University of Canterbury

Richard C. Zimmerman
Old Dominion University, rzimmerm@odu.edu

Follow this and additional works at: https://digitalcommons.odu.edu/oeas_fac_pubs

Part of the Oceanography Commons, Plant Sciences Commons, and the Terrestrial and Aquatic Ecology Commons

Original Publication Citation

RESEARCH ARTICLE

The vulnerability and resilience of seagrass ecosystems to marine heatwaves in New Zealand: a remote sensing analysis of seascape metrics using PlanetScope imagery

Ken Joseph E. Clemente[1,2] (iD), Mads S. Thomsen[1,3] (iD) & Richard C. Zimmerman[4] (iD)

[1]Marine Ecology Research Group, School of Biological Sciences, University of Canterbury, Christchurch 8041, New Zealand
[2]University of Santo Tomas, Manila 1015, Philippines
[3]Department of Bioscience, Aarhus University, 4000, Roskilde, Denmark
[4]Department of Ocean and Earth Sciences, Old Dominion University, Norfolk, Virginia 23529, USA

Abstract

Seagrasses are foundation species that provide ecosystem functions and services, including increased biodiversity, sediment retention, carbon sequestration, and fish nursery habitat. However, anthropogenic stressors that reduce water quality, impose large-scale climate changes, and amplify weather patterns, such as marine heatwaves, are altering seagrass meadow configurations. Quantifying large-scale trends in seagrass distributions will help evaluate the impacts of climate drivers on their functions and services. Here, we quantified spatiotemporal dynamics in abundances and configurations of intertidal and shallow subtidal seagrass (*Zostera muelleri*) meadows in 20 New Zealand (NZ) estuaries that span a 5-year period (mid/late 2016–early 2022) just before, during and after the Tasman Sea 2017/18 marine heatwave, the warmest summer ever recorded in NZ. We used high-resolution PlanetScope satellite imagery to map interseasonal seagrass extent and quantify seascape metrics across 20 estuaries along a latitudinal gradient spanning 12° in NZ. We also explored the association of changes in seagrass metrics with satellite-derived predictors such as sea surface temperature (SST), SST anomaly (SSTa), water column turbidity, and nutrient concentration. Our analyses revealed that NZ seagrass meadows varied in areal extent between years and seasons, but with no clear patterns over the 5-year period, implying resilience to large-scale stressors like the 2017/18 marine heatwave. Small-scale patterns were also dynamic, for example, patch sizes and patch configurations differed across estuaries, seasons, and years. Furthermore, seagrass patches expanded in some estuaries with increasing SST and SSTa. These results highlight dynamic seagrass patterns that likely affect local processes such as biodiversity and carbon sequestration. Our analyses demonstrate that a combination of high-resolution satellite remote sensing and seascape metrics is an efficient and novel approach to detect impacts from anthropogenic stressors, like eutrophication and climate changes, and climate extremes like cyclones and heatwaves.

Introduction

Seagrass meadows support a variety of ecosystem functions and services, such as provision of nursery habitat and breeding grounds for diverse fauna (Fortes, 2012), dampening coastal waves and stabilizing marine sediments (Orth et al., 2006), removing nutrients (McGlathery et al., 2007), and sequestering blue carbon (Howard et al., 2017). Seagrasses, however, are vulnerable to light reductions caused by eutrophication and sediment loading,

climate change, and marine heatwaves (Arias-Ortiz et al., 2018; Dunic et al., 2021; Marbà & Duarte, 2010; Robertson & Savage, 2021; Smale et al., 2019; Thomson et al., 2015). For example, substantial seagrass mortalities have been documented after marine heatwaves in iconic seagrass meadows, such as in Shark Bay, Western Australia (Strydom et al., 2020), the Mediterranean Sea (Jordà et al., 2012), and the Chesapeake Bay (Hammer et al., 2018; Moore et al., 2012; Moore & Jarvis, 2008). Given that extreme climatic events like marine heatwaves are expected to increase in the future, it is of paramount importance to understand how they affect seagrass meadows.

Zostera muelleri, the only seagrass in New Zealand (NZ), inhabits intertidal flats and shallow subtidal areas within estuaries (Graeme, 2012; Turner & Schwarz, 2006). Anthropogenic and natural disturbances and stressors to *Z. muelleri* sometimes cause patchy distributions and limit sexual reproduction and resilience (Dos Santos & Matheson, 2017). It has been suggested that *Z. muelleri* populations in NZ have declined in recent decades although their present and historical extent is inadequately documented, especially in relation to environmental stressors (Matheson, 2018). Still, recent observations suggest that *Z. muelleri* can recolonize lost patches and meadows in both estuarine mudflats and intertidal reefs on the North Island of NZ (Lundquist et al., 2018; Madarasz-Smith & Shanahan, 2020) but few studies have analyzed losses and/or recovery processes in the South Island. In the austral summer of 2017/18, much of the South Island experienced the strongest marine heatwave on record (Salinger et al., 2020) killing large numbers of intertidal *Durvillaea* spp. (southern bull kelp) (Thomsen et al., 2021) and subtidal *Macrocystis pyrifera* (giant kelp) (Tait et al., 2021), facilitating invasive species (Thomsen et al., 2019) and altering species diversity and species-interaction networks (Thomsen & South, 2019) on coastal rocky reefs. In contrast, the effects of marine heatwaves on *Z. muelleri* meadows have not been studied in NZ even though heatwaves have grown stronger, longer, and more frequent over the past decade (Salinger et al., 2020; Tait et al., 2021; Thomsen et al., 2019). Simulations of heatwaves in laboratory experiments suggest that *Z. muelleri* responds with reduced photophysiological functioning and is less tolerant to warm anomalous events compared with other seagrass species (Nguyen, Bulleri, et al., 2021). However, exposure to a second heatwave improved the physiological performance of *Z. muelleri* through thermal priming (Nguyen et al., 2020). These conflicting results make it difficult to understand or predict the response of *Z. muelleri* meadows, under natural conditions, to marine heatwaves in NZ.

Repeated mapping of seagrass meadows is essential to document changes and better understand their spatiotemporal dynamics in response to stress factors such as marine heatwaves. Robust measures for assessing spatial change in seagrass meadows include quantifying changes in seascape metrics (the marine equivalent to terrestrial landscapes metrics, Table S1). For example, studies that used seascape metrics have identified mechanisms of losses from time series analysis of patch configuration (Kaufman & Bell, 2022), linked seagrass seascape configuration and complexity to conservation and environmental changes (Arellano-Méndez et al., 2019), and linked facilitation processes, habitat connectivity and aggregation of seagrass patches (Cuevas et al., 2021). Analyzing seascape metrics could therefore increase sensitivity to detect impacts from extreme events, enable fine-scale detection of changes associated with environmental stressors, and provide better ecological understanding of seagrass dynamics.

Recent advances in satellite remote sensing imagery permit detailed analysis of seascape metrics at scales not possible with traditional ground-based mapping efforts. Remote sensing is potentially a useful tool because it can be done on large scales covering entire meadows within and across estuaries, using retrospective data collections (e.g., analyzing images from before, during, and after a heatwave) and allowing for repeated measurements to separate directional and cyclic changes. High-resolution satellite imagery such as PlanetScope (3 m pixel multispectral resolution) is promising for seagrass detection because of its high (daily) temporal coverage (Wicaksono et al., 2022), which increases the probability of acquiring images taken at low tide and on cloud-free days for better analysis of intertidal seagrass cover. Remote sensing analysis combined with environmental predictors and seagrass seascape metrics should be a valuable tool to inform seagrass management policies. The aims of this study were therefore: (i) to exploit seagrass seascape metrics in 20 estuaries in NZ spanning a 12° latitudinal gradient to quantify temporal trends over a 5-year period that included the Tasman Sea 2017/18 marine heatwave and (ii) to determine whether large climate drivers such as sea surface temperature (SST), SST anomalies, and other predictors like water clarity and nutrients could be related to changes in spatial seascape metrics in seagrass meadows. More specifically, we hypothesized that *Z. muelleri*, like other seagrasses, would be negatively affected by extreme marine heatwaves and that impacts would be more severe in northern warmer estuaries (Arias-Ortiz et al., 2018; Marbà & Duarte, 2010; Smale et al., 2019; Thomson et al., 2015).

Materials and Methods

Study sites

Twenty estuaries across NZ were selected (Fig. 1) based on available prior data from geotagged photographs and
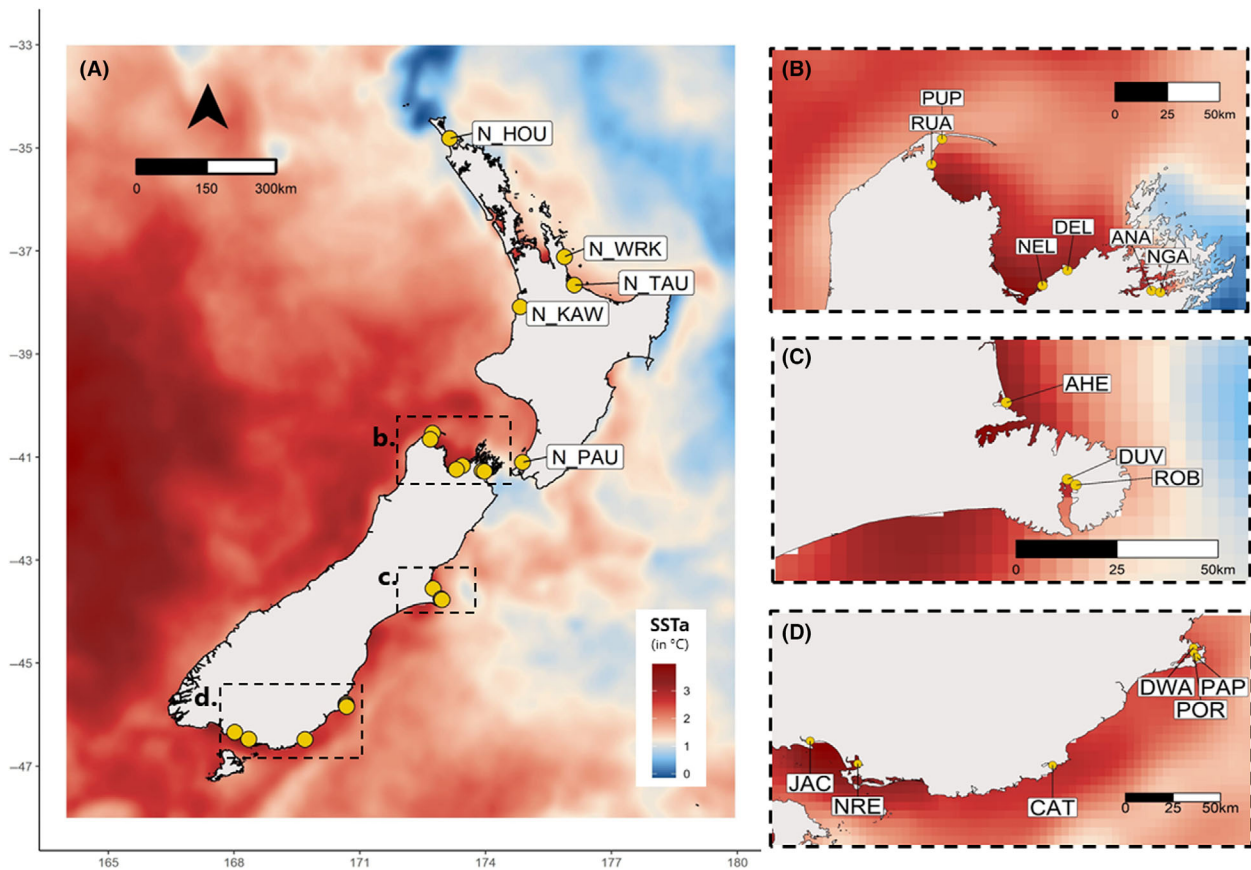
Figure 1. Maps of estuaries in New Zealand, analyzed for seagrass cover and patch dynamics with satellite images, including (A) overview of all 20 estuaries where five are from the North Island (outside dashed boxes) and 15 from (B) northern, (C) central, and (D) southern regions of South Island (dashed boxes and insets). The estuaries are superimposed on a heat map showing monthly sea surface temperature anomaly (SSTa) in January 2018, the hottest month during the extreme 2017/18 Tasman Sea marine heatwave. SSTa was based from NOAA Coral Reef Watch Monthly Global 5 km grid data (2018).

drone images and literature that reported *Z. muelleri* occurrences (Table S2). The 20 estuaries were situated along a gradient spanning 12° of latitude, and they experienced the 2017/18 marine heatwave to different degrees (Fig. 1). In addition to different temperature regimes, the 20 estuaries also represented a wide range of *Z. muelleri* meadow sizes and patch configurations (Figure S5), tidal ranges, and anthropogenic stressors (Table 1).

Satellite image acquisition

To test for temporal trends in seagrass cover and possible links to large-scale temperature stressors, satellite images were analyzed for a period of *c.* 5 years from mid-late 2016 to early 2022. Images were sourced from the Planet-Scope Dove satellite constellation from the PSScene4Band Sensor (PS4) with pixel resolution of *c.* 3 m (nadir viewing) (Planet Team, 2018). Using such high spatial

resolution allows for improved seagrass patch dynamic analysis (Hill et al., 2014) that is particularly important when quantifying fragmented seagrass meadows of relatively small species, like *Z. muelleri* (McKenzie et al., 2022). To get the best possible images for analyses, temporal coverage was restricted to one image per season (four images per year), generating 22 images per estuary – including 20 images covering 2017–2021, one image from 2016 to get best possible before heatwave data (PlanetScope launched in June 2016) and one image from early 2022 to cover the 2021/22 summer that also was unusually hot. A few estuaries did not have the complete set of 22 images due to cloud cover, water column turbidity, tide stage or lack of satellite pass. The screening criteria for satellite images include <10% cloud cover, minimal water turbidity, zero to minimal glint, and temporal proximity to local low tide times modeled by NIWA (www.tides.niwa.co.nz). All sourced images were

Table 1. Key characteristics of 20 estuaries in New Zealand, analyzed for seagrass cover and patch dynamics with satellite images, including SST and SST anomaly means for 2017–2021, their estuary trophic index (ETI) susceptibility rating, and ecological stress based on ETI macroalgae susceptibility band.

Estuary	Site ID	Latitude	Longitude	Estuary type[a]	Spring tidal range (m)[a]	5-year mean SST (°C)[b]	5-year mean SSTa (°C)[b]	ETI susceptibility[c]	Likely stress from macroalgae[c]
North Island									
Houhora	NHOU	−34.815	173.137	Shallow drowned valley	2.0	18.08	0.70	Moderate	Minor
Wharekawa	NWRK	−37.113	175.874	Tidal lagoon	1.7	17.93	0.73	Moderate	Minor
Tauranga	NTAU	−37.659	176.114	Shallow drowned valley	1.7	17.62	0.75	Moderate	Minor
Kawhia	NKAW	−38.084	174.820	Shallow drowned valley	3.0	17.12	0.64	Low	None
Pāutahanui	NPAU	−41.097	174.877	Shallow drowned valley	1.0	15.52	0.83	Moderate	Minor
North of South Island									
Puponga Bay	PUP	−40.533	172.733	Tidal lagoon	3.7	15.61	0.56	Low	None
Ruataniwha Inlet	RUA	−40.654	172.674	Tidal lagoon	3.7	15.56	0.52	High	Moderate
Delaware Inlet	DEL	−41.167	173.441	Tidal lagoon	3.5	16.00	0.81	Low	None
Nelson Haven	NEL	−41.240	173.300	Tidal lagoon	3.6	16.06	0.92	Low	None
Anakiwa Bay	ANA	−41.265	173.916	Deep drowned valley	1.5	14.88	0.53	Low	None
Ngakuta Bay	NGA	−41.273	173.965	Deep drowned valley	1.5	14.88	0.53	Low	None
Central of South Island									
Avon Heathcote	AHE	−43.550	172.745	Tidal lagoon	1.8	13.65	0.99	High	Moderate
Duvauchelle Bay	DUV	−43.753	172.934	Deep drowned valley	1.8	13.24	0.75	Moderate	None
Robinsons Bay	ROB	−43.768	172.960	Deep drowned valley	1.8	13.24	0.75	Moderate	None
South of South Island									
Waipuna Bay	WAI	−45.789	170.664	Deep drowned valley	1.6	12.57	0.84	Low	None
Portobello Bay	POR	−45.822	170.666	Deep drowned valley	1.6	12.57	0.84	Low	None
Papanui Inlet	PAP	−45.847	170.686	Tidal lagoon	1.6	12.51	0.88	Moderate	Minor
Jacob River Estuary	JAC	−46.341	168.015	Tidal lagoon	2.3	12.97	0.63	Very high	Significant
New River Estuary	NRE	−46.475	168.343	Shallow drowned valley	2.2	12.93	0.71	Very high	Significant
Catlins River Estuary	CAT	−46.484	169.690	Tidal lagoon	1.8	12.47	0.97	High	Moderate

[a]Data based on Hume et al. (2016).
[b]Satellite-derived annual mean sea surface temperature (SST) and SST anomaly based on the nearest oceanic pixels from estuary opening.
[c]Ratings per estuary were based on the web tool for ETI Tool 1 (Zeldis et al., 2017) and interpreted according to Robertson et al. (2016).

downloaded as orthorectified, radiometrically calibrated, atmospherically corrected, and Sentinel-harmonized surface reflectance (SR) products (Planet Team, 2022).

Satellite image classification

The SR products from PS4 scenes were visually examined and checked for spectral signatures prior to identifying training sites for supervised classification. The training sites were identified by examining the spectral information contained in the training patches (Coffer et al., 2020; Lebrasse et al., 2022) combined with georeferenced information from drone and photo images taken by co-author Thomsen and colleagues in South Island sites, literature-reported seagrass maps for both North and South Island sites (Table S2), or expert knowledge derived from field surveys (Thomsen, pers. obs.). Training classes consisted of 'seagrass', 'sediment', and 'water'. Land pixels with positive elevation identified using digital elevation models downloaded from LINZ Data Service (http://data.linz.govt.nz) were removed prior to classification analysis. The time series images from each site were trained and batch-classified using the Support Vector Machine (SVM) algorithm implemented in ArcGIS Pro (Munir & Wicaksono, 2019; Traganos & Reinartz, 2018). SVM – a supervised machine learning method that classifies pixel-based multiband imagery from an input training dataset – is a common and reliable mathematical algorithm for seagrass classification (Chandra & Bedi, 2021; Traganos et al., 2018; Widya et al., 2023). Specifically, SVM finds the optimal hyperplane (boundary) that separates different feature classes from the maximum margin between closest points, a well-established method to detect complex decision boundaries from relatively few training data (Drucker et al., 1996). Because the seagrass cover was temporally dynamic, some of the training patches had to be repositioned from image to image for the same location to achieve accurate classification. The classified raster image outputs were postprocessed by reclassifying them into 'seagrass' and 'non-seagrass' classes only. Raster maps were also 'cleaned' using the shrink feature in ArcGIS that removes isolated 'noisy' pixels (Enwright et al., 2022). Training patches were created manually for each image in ArcGIS Pro. Classification of the entire image library was automated using the Python 'arcpy' library.

Classification agreement was assessed by first generating equalized random accuracy points derived from the reference photograph and drone images that were not used during model training (note that we used an average of 63% and 37% for training and validation, respectively). We also compared our classification maps to literature-reported seagrass maps that were georeferenced, rasterized, resampled, and reprojected to attributes

similar to the classified raster images (Chiang et al., 2014). This method is relatively similar to Lebrasse et al. (2022) and Coffer et al. (2020) that performed agreement assessment between classified satellite images and aerial images. Comparing our classification to the rasterized literature maps (which are primarily derived from aerial imagery and field surveys, Table S2) is more robust as it covers the same area as our area of interests than the fewer rasterized points from photographs and drones. Only classified images that closely coincided with the reference dates were selected for agreement assessment (Table 2). Confusion matrices were then calculated to generate agreement statistics (Table 2). Note that we used the term agreement throughout instead of accuracy because the reference datasets were imbalanced and do not always contain observations that were independently validated (i.e., accuracy is not always guaranteed) (Coffer et al., 2023). We also investigated the potential influence of tidal height at the time of satellite image capture on the seagrass cover detected by our classification process. We performed regression analyses between seagrass canopy area estimates and the tidal heights acquired from NIWA across the entire time series and for each site. We also checked for assumptions of normality and homoscedasticity and implemented data transformation (Tukey's Ladder of Powers) where necessary. Agreement between satellite date and ground-based data products, and tidal height sensitivity analyses, were done in ArcGIS Pro and R studio (R Core Team, 2021; RStudio Team, 2021), respectively.

Seascape metrics analysis

The application of seascape metrics to remote sensing classification provides a broader level of quantitative technique for seagrass monitoring than conventional pixel-by-pixel quantification (Baumstark, 2018). Here, we used the seagrass raster maps to calculate seascape metrics and assess changes in seagrass meadow configuration over time. Our study targeted seagrass dynamics, and we therefore selected the subset of class-level metrics that accounted for total extent, and the size, fragmentation, and connectivity of seagrass patches (Hesselbarth et al., 2019; McGarigal et al., 2012) – metrics that have ecological implications, for example, for seagrass-associated animal population dynamics and species interactions (Uhrin & Turner, 2018). Seascape metrics included: total class area (CA), mean patch area (AREA_MN), number of patches (NP), total class edge (TE), patch cohesion index (COHESION), and largest patch index (LPI). For details on these metric, please see summary Table S1 and Hesselbarth et al. (2019). Spatial metrics were calculated using the 'landscapemetrics'

Table 2. Agreement assessment results per site.

Site	Reference data used	Reference date	Satellite image date	P_accuracy non-seagrass	P_accuracy seagrass	U_accuracy non-seagrass	U_accuracy seagrass	Overall accuracy	Kappa coefficient
AHE	Rasterized map	2016-Mar	2016-Nov	0.86	0.87	0.88	0.86	0.87	0.74
DUV/ROB	Drone/Photographs	2020-Jul	2020-Jul	1.00	0.52	0.67	1.00	0.76	0.52
DWA	Photographs	2016-Oct	2016-Sep	1.00	0.75	0.86	1.00	0.90	0.78
	Drone/Photographs	2020-Jul	2020-Aug	1.00	0.72	0.78	1.00	0.86	0.72
POR	Photographs	2020-Jul	2020-Aug	0.694	1.00	1.00	0.58	0.78	0.57
PAP	Photographs	2016-Oct	2016-Sep	0.93	0.6	0.7	0.9	0.77	0.53
	Rasterized map	2021-Nov	2021-Oct	0.81	0.83	0.84	0.80	0.82	0.64
CAT	Rasterized map	2016-Dec	2016-Dec	0.80	0.72	0.68	0.84	0.76	0.52
NRE	Rasterized map	2016-Feb	2016-Sep	0.73	1.00	1.00	0.64	0.82	0.64
JAC	Rasterized map	2016-Feb	2017-Feb	0.77	0.94	0.96	0.72	0.84	0.68
NGA	Photographs	2016-Apr	2016-Sep	1.00	0.67	0.875	1.00	0.90	0.74
	Rasterized map	2018-Mar	2018-Feb	0.78	0.92	0.93	0.74	0.83	0.67
ANA	Rasterized map	2018-Mar	2018-Jan	0.93	0.87	0.87	0.93	0.90	0.80
DEL	Photographs	2016-Apr	2016-Nov	1.00	0.75	0.86	1.00	0.90	0.78
	Drone/Photographs	2020-Jun	2020-Aug	1.00	0.79	0.83	1.00	0.89	0.79
NEL	Photographs	2020-Jun	2020-Aug	1.00	0.82	0.82	1.00	0.90	0.80
RUA	Rasterized map	2015-Mar	2016-Nov	0.81	1.00	1.00	0.76	0.88	0.76
	Photographs	2016-Apr	2016-Nov	1.00	0.80	0.83	1.00	0.90	0.80
PUP	Photographs	2016-Apr	2016-Sep	1.00	0.69	0.64	1.00	0.80	0.61
NPAU	Rasterized map	2020-Jan	2020-Feb	0.84	0.91	0.92	0.82	0.87	0.74
NKAW	Rasterized map	(?)2011	2017-Jan	0.70	0.82	0.86	0.64	0.75	0.50
NTAU	Rasterized map	2011	2016-Sep	0.72	0.97	0.98	0.62	0.80	0.60
NWRK	Rasterized map	2017/18-SUM	2018-Feb	0.70	0.88	0.92	0.60	0.76	0.52
NHOU	Spectral info only	2022-Jan	2022-Jan	1.00	0.82	0.81	1.00	0.90	0.80

See Table 1 for details and abbreviations of individual estuaries.

No available literature map can be rasterized for NHOU, but we refer to image and textual information from reference in Table S2.

package (Hesselbarth et al., 2019) in R studio (R Core Team, 2021; RStudio Team, 2021).

To detect whether there were monotonic temporal increases or decreases in seagrass seascape metrics among sites from 2016 to 2022, we ran seasonal Kendall (SK) tests (Helsel et al., 2020; Hirsch & Slack, 1984) – an extension of traditional Mann-Kendall trend tests (Kendall, 1938; Mann, 1945). These tests ran the traditional Mann-Kendall Test separately in each of the seasons (e.g., our summer data were only compared with other summer data in the time series) (Helsel & Frans, 2006). An overall SK statistic was generated by combining individual SK statistics for each season to derive Kendall's tau correlation coefficient (τ) that measures the strength of the monotonic relationship between time and test variables (Helsel & Frans, 2006). We calculated the trend slope, τ, and P-values to evaluate the probability that there were no trends in all analyzed seascape metrics in each estuary. Following Lebrasse et al. (2022), we interpreted τ coefficients as in Cohen (1988), where an absolute value of $0.1 \leq \tau < 0.3$, $0.3 \leq \tau < 0.5$, and $0.5 \leq \tau < 1$ is considered a weak, moderate, or strong trend, respectively. The SK trend tests were performed using the 'rkt' package (Marchetto & Marchetto, 2021) in R studio (R Core Team, 2021; RStudio Team, 2021).

Environmental predictors analysis

We explored the potential association of large-scale climate drivers such as nearby oceanic SST, SST anomaly (SSTa), turbidity, and water column chlorophylls with seagrass seascape metrics. Monthly estimates of SST and SSTa from June 2016 to February 2022 were downloaded from NOAA Coral Reef Watch Monthly Global 5 km resolution datasets (2018). These monthly estimates were based on the oceanic pixels nearest the mouth of the estuaries supporting seagrass meadows (see Figure S4 for pixels position). We also tested whether the seagrass metrics were sensitive to other satellite-derived water quality predictors relevant to seagrass performance such as light attenuation [K_d490 (Sully & van Woesik, 2020)] and nutrient limitation [proxied by Chlorophyll-a concentration (Veettil et al., 2020)]. Monthly values of both K_d490 and Chl-a were obtained from the NASA OceanColor database (https://oceandata.sci.gsfc.nasa.gov/) using MODIS-Aqua Global 4 km Science Quality monthly composite datasets. These data were taken from the same pixel location as in the SST data (except for two sites that were further in from the ocean and were not covered by MODIS). High-quality in situ measurements for the water quality predictors did not exist for all 20 estuaries; hence for consistency, we used standardized satellite-derived data mostly from the nearest offshore pixels (Figure S4),

assuming a linkage between the ocean and the estuary through tidal mixing (Newton & Mudge, 2003; Sims et al., 2022).

Monthly data of all predictors were filtered to match the corresponding months of seagrass cover across the time series. The potential effects of monthly SST, SSTa, K_d490, and Chlorophyll-a on seagrass seascape metrics were analyzed with multiple linear regression (MLR). MLR is widely used to detect associations between environmental predictors and seagrass response metrics (Lebrasse et al., 2022; Pansini et al., 2021; Tuya et al., 2013; Unsworth et al., 2007). All seascape metrics data were automatically transformed using Tukey's Ladder of Powers approach (Tukey, 1977) prior to running MLR analyses. All workflow for environmental predictors was done in R studio (R Core Team, 2021; RStudio Team, 2021), using the 'rerddap' package (Chamberlain, 2021) for fetching satellite data from the NOAA ERDDAP server, and the 'rcompanion' package (Mangiafico, 2022) for data transformation.

Results

We analyzed a total of 449 satellite images from 20 estuaries in NZ spanning the period from austral Spring 2016 to Summer 2021/22. Our analysis did not show clear long-term monotonic trends in total seagrass extents across all estuaries, and patch metrics often fluctuated in sizes and configuration across estuaries, latitudes, seasons and with water temperature. The classification process had an overall agreement that ranged from 75 to 90% and corresponding Kappa coefficients ranging from 0.52 to 0.80 (Table 2). Remote detection of seagrasses in all images and sites was not biased by tidal height at the time of satellite image capture (Figure S1).

Seascape metrics

For brevity, we focused here on results from estuaries with evident trends in total seagrass areal extent (class area) or those with a combination of three or more evident trends in other metrics (by assuming this as strong demonstration of patch dynamics). The analyses revealed no monotonic trends in seagrass class area in 18 of the 20 estuaries analyzed here across the +5 years as the slopes were not different from zero ($P > 0.05$, Fig. 2A). Only two estuaries, Nelson Haven and Duvauchelle Bay on the South Island, exhibited strong and moderate increases in class area ($\tau = 0.51$ and 0.46, $P = 0.02$ and 0.02, $n = 22$ and 22, respectively, Fig. 2A). However, seagrass area was highly variable across seasons and years in most estuaries (Fig. 3). Some estuaries, including Nelson and Duvauchelle, varied significantly in other seascape metrics,
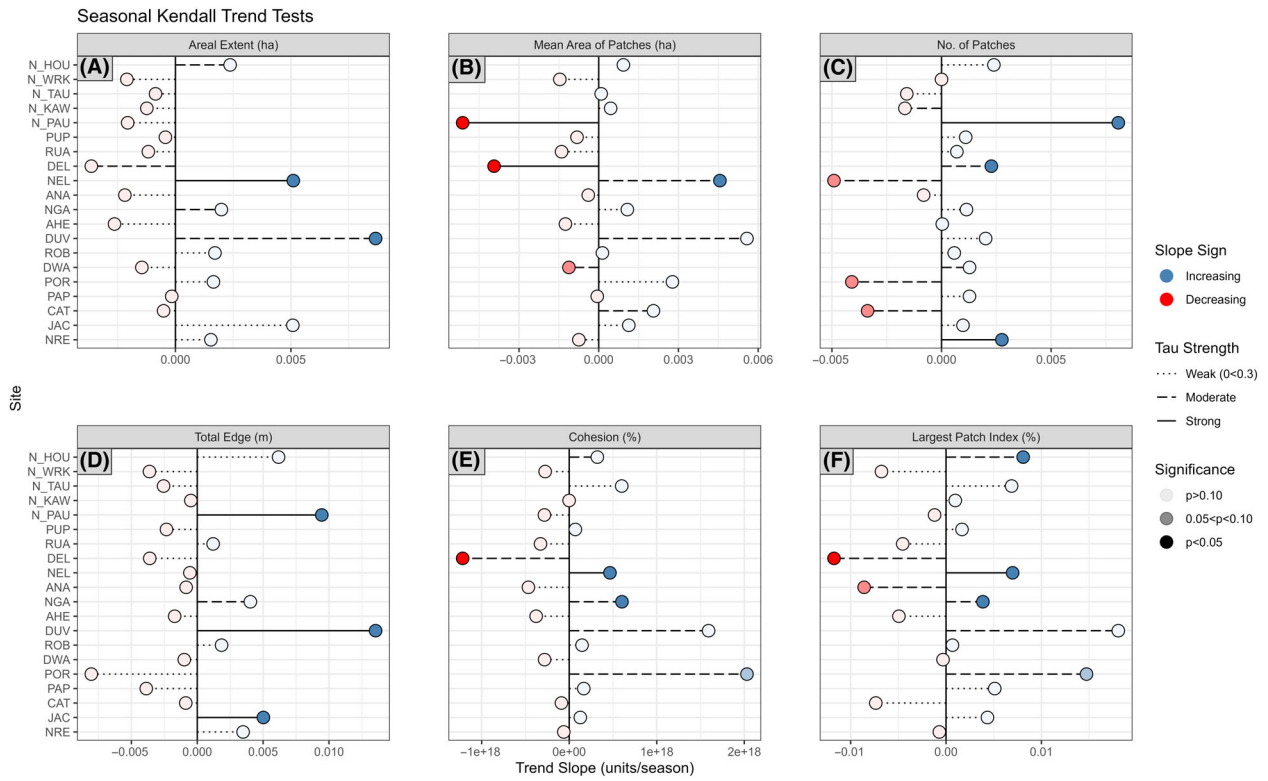
Figure 2. Summary of Seasonal Mann-Kendall trend tests (slopes) of six seascape metrics (A–F) for 20 estuaries arranged from northern (top) to southern (bottom) latitudes across seasons from Spring 2016 to Summer 2021/22. See Table 1 and Figure 1 for details and abbreviations of individual estuaries.
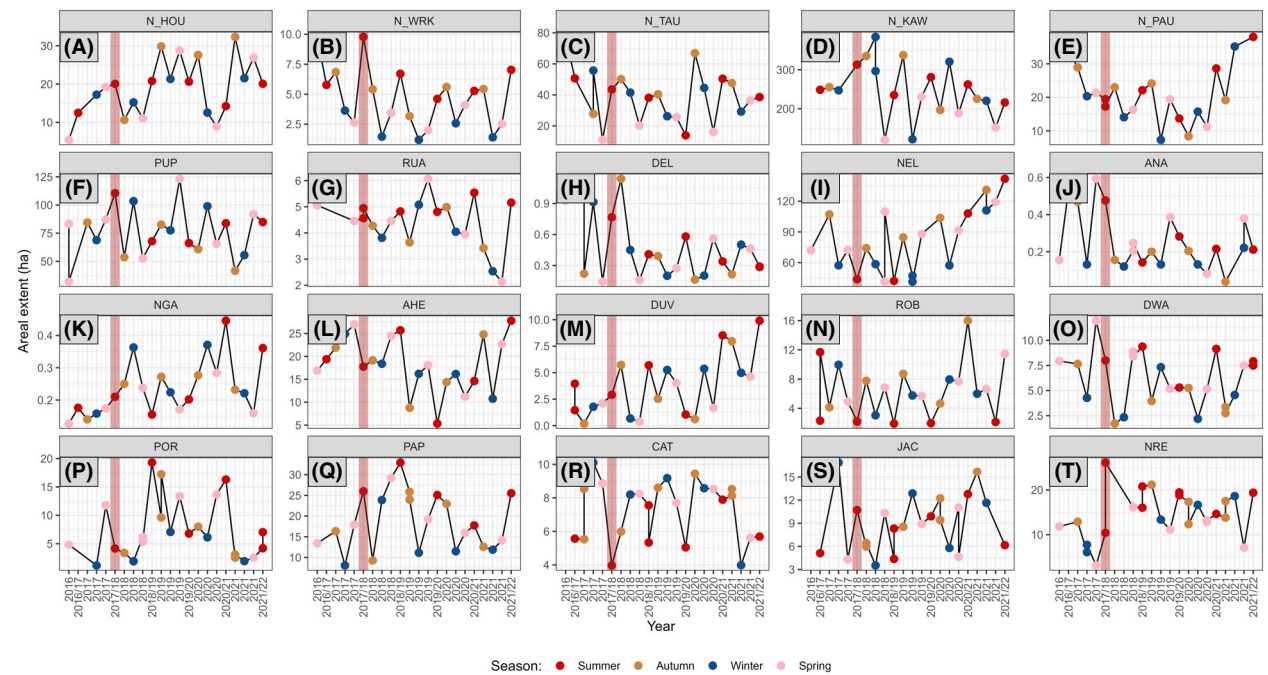

Figure 3. Seagrass areal extent for 20 estuaries (A–T) arranged from northern (top) to southern (bottom) latitudes across the time series where points are colored according to seasons. See Table 1 and Figure 1 for details and abbreviations of individual estuaries. Red box indicates data during 2017/18 marine heatwave.

demonstrating high patch dynamics. Although total seagrass area in Pāutahanui in North Island appeared constant over time, patch fragmentation increased as indicated by a decrease in mean patch area ($\tau = -0.51$, $P = 0.02$, $n = 22$, Fig. 2B), increase in patch number ($\tau = 0.80$, $P < 0.01$, Fig. 2C) and total edge length ($\tau = 0.51$, $P = 0.02$, Fig. 2D). In contrast, the temporally stable class area in Delaware Bay on South Island was accompanied by a decrease in mean patch area ($\tau = -0.52$, $P < 0.01$, $n = 23$, Fig. 2B) and in largest patch index ($\tau = -0.40$, $P = 0.045$, Fig. 2F). There was also an indication of fragmentation in Delaware due to moderate trends in both number of patches ($\tau = 0.46$, $P = 0.02$, Fig. 2C) and cohesion ($\tau = -0.40$, $P = 0.045$, Fig. 2E). The significant increase in class area observed in the Nelson Estuary was accompanied by moderate increase in mean patch area, a strong increase in largest patch index, and likely patch aggregation due to a strong increase in cohesion. However, the increase in class area observed in Duvauchelle Bay was not coupled with any trends in patch configuration except for a strong increase in total edge, which is also indicative of fragmentation. Other trends were unique for some estuaries by having one or two significant or near significant slopes among the analyzed metrics (Fig. 2). Although there were few temporal trends in total cover over the five-year period, seagrass was more abundant in summer than winter in NZ estuaries (14 estuaries increased by *c.* 63% vs. 6 decreased by *c.* 15%, Table S3). This seasonal pattern was particularly strong in five of the estuaries (see Fig. 3B,J,O, P,Q) where seagrass cover, on average, increased by >80% from winter to summer (Table S3).

Environmental drivers

Multiple linear regressions quantified the associations between monthly SST and SSTa and various seagrass seascape metrics for several estuaries (Figs. 4 and 5). However, monthly Chlorophyll-*a* and K_d-490 had poor explanatory power across seascape metrics, sites, and time series with highly variable regression slopes and $P > 0.10$ (Figures S2 and S3). Furthermore, while SST and SSTa were important warming predictors, they did not exhibit uniform effects across estuaries. For example, there was significant effect of SST but not SSTa on seagrass metrics in Papanui Inlet. In contrast, there was a nonsignificant SST and significant SSTa on seagrass meadows in Avon Heathcote Estuary (Figs. 4 and 5). We therefore here present their effects separately.

Specifically, we found a decreasing trend ($-\beta$) for number of patches with SST but positive trend ($+\beta$) between SST and class area, mean patch area, cohesion, and largest patch index (Fig. 4). These patterns suggest that seagrass expansion and patch aggregation generally increased, and meadow fragmentation decreased with temperature, as demonstrated in estuaries such as Wharekawa, Nelson, and Papanui (although in Nelson, patch numbers appeared constant, Fig. 4C). This pattern potentially also existed for Ruataniwha where similar direction of slopes was evident for cohesion and largest patch index (Fig. 4). Moreover, New River Estuary also showed association between SST and seagrass expansion for class area and mean patch area but did not drive other patch configurations (Fig. 4C–F).

By comparison with SST, association between SSTa on seascape metrics was less common and varied more across estuaries. For example, in Nelson, increases in SSTa tended to decrease seagrass class area, mean patch area, cohesion, and largest patch index (i.e., indicative of patch contraction and fragmentation, Fig. 5). This pattern was relatively similar for Ruataniwha where four metrics also decreased although only near-significantly so for class area, mean patch area, and cohesion (Fig. 5A,B,E,F). Interestingly, we found positive association between SSTa and seagrass class area, total edge, and largest patch index in the Avon Heathcote estuary (Fig. 5A,D,F). Other trends included a positive association between SSTa and mean patch area but negative with total edge in Wharekawa (Fig. 5B,D) and decreasing mean patch area with SSTa in New River Estuary (Fig. 5B).

Discussion

Remote sensing detection of seagrasses has been widely used for management and monitoring of local systems but rarely on a larger scale and wider ecological seascape context. Our study is, as far as we know, the first to utilize PlanetScope's high-resolution satellite imagery to detect trends across fine temporal (intraannual/interseasonal) and wide geographic (20 estuaries along a 12° latitudinal gradient) scales, compared with more common interannual and/or single-site studies. The relations between seascape metrics and climate variables presented here also remain relatively rare in seagrass remote sensing studies. By combining satellite-based methods with seascape metrics, we documented that *Z. muelleri* meadows fluctuated considerably across seasons in NZ estuaries, without any clear monotonic trends of long-term losses or gains, and that seagrass patches expanded significantly in some estuaries with increasing SST and SST anomalies. In other words, we did not find support for our initial working hypothesis that *Z. muelleri* would be severely inhibited by heatwaves. Instead, our results suggest that *Z. muelleri* is resilient to large-scale stressors like the extreme 2017/18 marine heatwave and may be responding positively to climate warming that has potential cascading
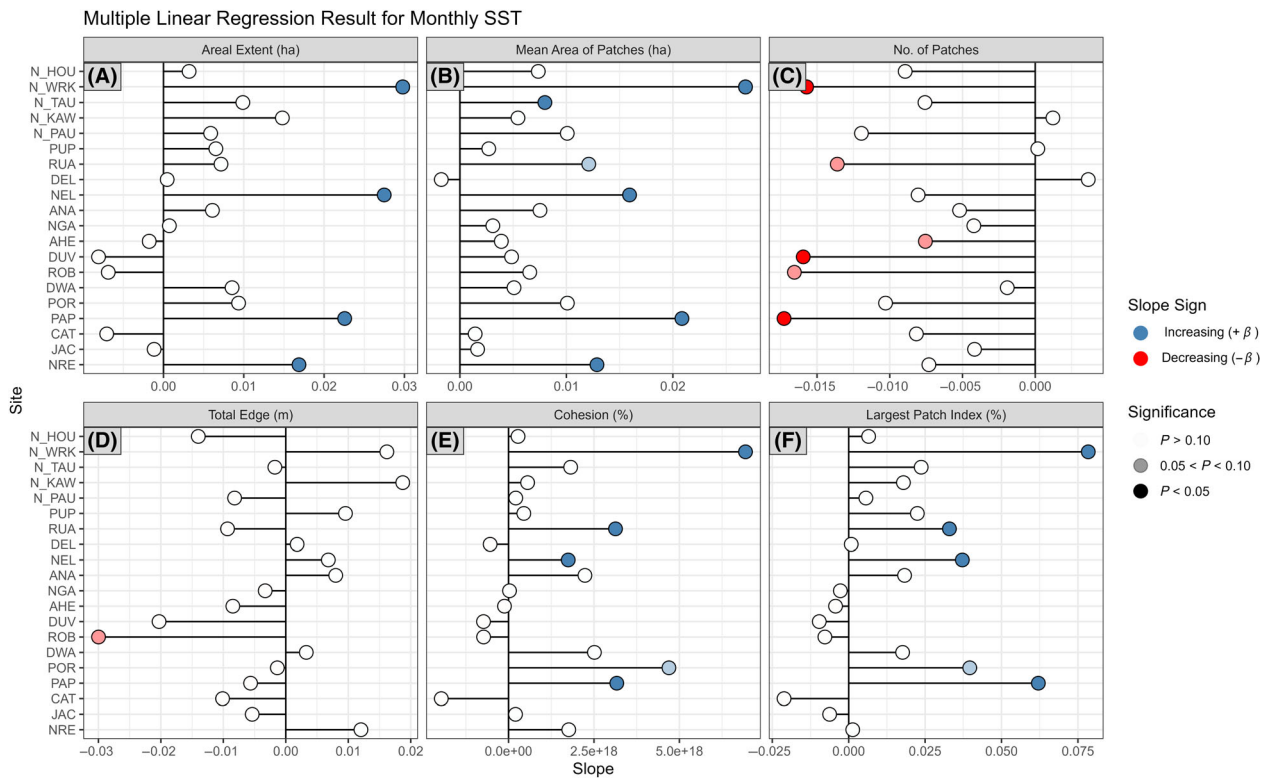
Figure 4. Summary of multiple linear regression tests (slopes) of six seascape metrics (A–F) versus monthly SST for 20 estuaries arranged from northern (top) to southern (bottom) latitudes. See Table 1 and Figure 1 for details and abbreviations of individual estuaries. SST, sea surface temperature.

effects on other ecosystem services provided by seagrass meadows.

Seagrass seascape metrics

Here, using remotely sensed data, we quantified seagrass patch dynamics, which are extremely difficult to detect using ground-based measures of seagrass extent across the estuarine landscape. Specifically, the lower seagrass cover in winter months we found in some estuaries (Fig. 3; Table S3) is consistent with results from Ramage and Schiel (1999) where *Z. muelleri* patches decreased in size during winter. Although our findings suggest that there were no general increases or decreases in *Z. muelleri* extent over the last 5 years, there is evidence of patch-level variability and seasonal dynamics that potentially affect ecosystem function (Yarnall et al., 2022). Such variation in patch sizes, configurations, and connectedness can potentially affect meadow-scale processes including faunal recruitment, diversity, community structure, facilitation, predation, and hydrodynamics (Bryan et al., 2007; Turner et al., 1999). For example, fragmented *Z. muelleri* patches in NZ typically have lower density and richness

of faunal assemblages when compared to continuous meadows (Mills & Berkenbusch, 2009), and *Z. muelleri* expansion or recolonization can increase animal diversity (Lundquist et al., 2018). Dense cover in *Z. muelleri* meadows has also been linked to higher densities of grazers and predators (Alfaro, 2006), and patch fragmentation can increase predation rates (Irlandi et al., 1995). In addition to direct ecological effects, *Z. muelleri* patch dynamics (in contrast to bare sediments) can also modify local hydrodynamic conditions which again affects nutrient uptake (Bryan et al., 2007) larval settlement (Grizzle et al., 1996) and carbon sequestration (Lavery et al., 2013). Our analyses could therefore be useful to infer ecological consequences on both short-term seasonal scales and to interpret long-term changes to seagrass-associated communities.

Environmental predictors

The different spatiotemporal patterns in patch metrics observed across 20 NZ estuaries may be related to different underpinning abiotic and/or biotic drivers with subsequent differential impacts on the seagrass meadows (Bell
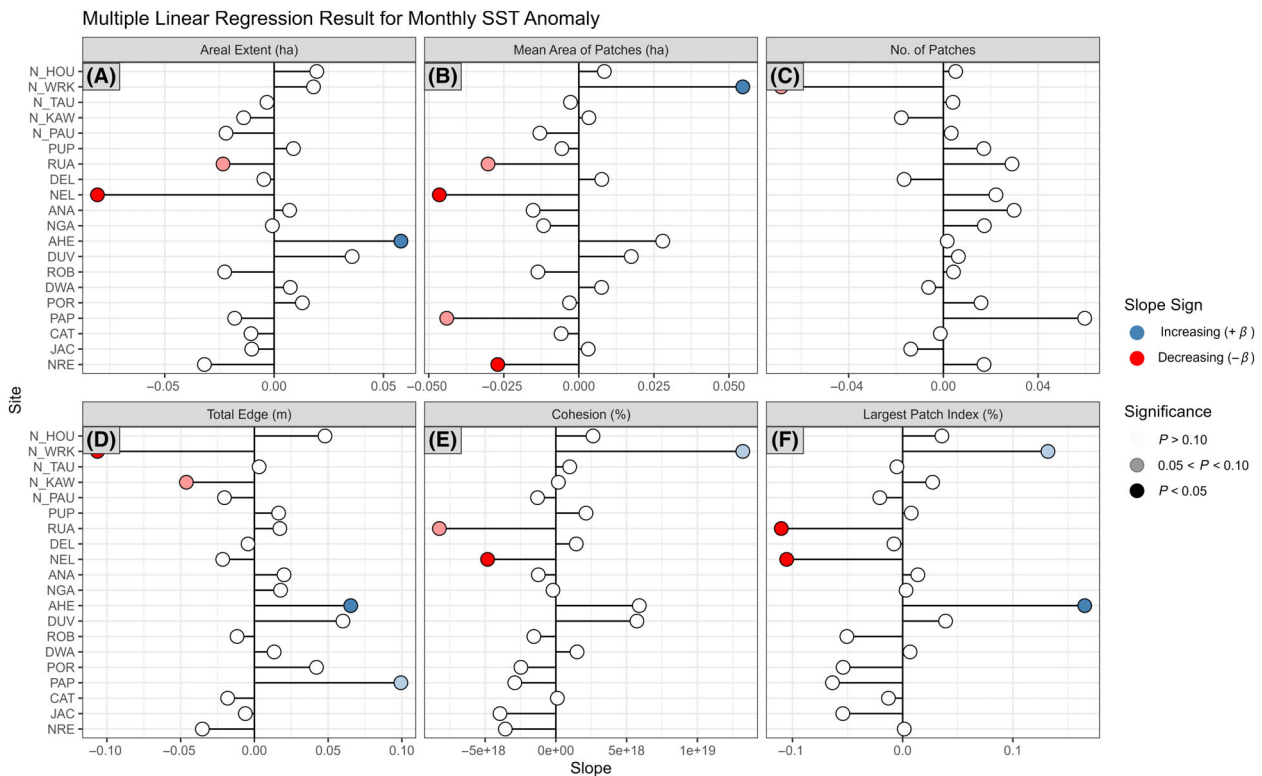
Figure 5. Summary of multiple linear regression tests (slopes) of six seascape metrics (A–F) versus monthly SST anomaly for 20 estuaries arranged from northern (top) to southern (bottom) latitudes. See Table 1 and Figure 1 for details and abbreviations of individual estuaries. SST, sea surface temperature.

et al., 2007). Possible biological drivers of seagrass patch dynamics, for example, associated with facilitation, herbivory, or diseases, cannot be measured from satellite images, in contrast to many potential physicochemical drivers, like SST, SSTa, chlorophyll and light attenuation.

We found no clear relationships between seagrass metrics and nearby oceanic Chlorophyll-a or light attenuation, perhaps because intertidal *Z. muelleri* are less affected by light limitation (Bulmer et al., 2016; Kohlmeier et al., 2014; Petrou et al., 2013; Schwarz, 2004; Zabarte-Maeztu et al., 2020). Alternatively, suspended sediment and phytoplankton concentrations could be disconnected from small-scale local estuarine water characteristics. However, standardized small-scale light attenuation and chlorophyll data do not exist for all 20 estuaries studied here, so our water quality tests were limited to oceanic satellite datasets. By contrast, we found several significant associations between nearby oceanic warming and seagrass seascape metrics. Although the analyses did not show clear consistent large-scale losses (or gains) of *Z. muelleri* linked to extreme heatwaves, as observed in other seagrass species (Jordà et al., 2012; Strydom et al., 2020), the warming predictors did affect many

Z. muelleri patch metrics. Specifically, our findings from some estuaries showed increases in aggregation and expansion of seagrass extent with increasing SST, which is consistent with past observed expansion of *Z. muelleri* during warmer months (Chartrand et al., 2016). This positive relationship is likely because *Z. muelleri* is living below its thermal optima for gross photosynthesis at 31°C (Collier et al., 2017) and vegetative growth at 27°C (York et al., 2013) throughout much of NZ.

Furthermore, SSTa, which is strongly related to marine heatwaves, rarely related with loss of seagrass extent, suggesting a lack of negative effects from more abrupt and short temperature spikes. Previous laboratory studies of *Z. muelleri* have demonstrated strong resilience to high temperatures, such as the ability to maintain productivity at 35°C (Collier et al., 2018), tolerance up to 30°C before biomass reduction (York et al., 2013) or tolerance up to 33°C before photosynthetic deterioration (Collier et al., 2011). In concert, our results combined with past findings suggest that *Z. muelleri* meadows in NZ may increase in extent under future warmer conditions, particularly in central and southern NZ (assuming other stressors, like eutrophication, do not increase), as also

demonstrated and predicted for Australian populations (Collier et al., 2018; Nguyen et al., 2020). More generally, future warming and stronger heatwaves will likely cause 'tropicalization' of NZ estuaries, bringing new winners and losers (e.g., of facilitators, herbivores and diseases) and may thereby cause cascading seagrass reconfigurations (Hyndes et al., 2017; Nguyen, Ralph, et al., 2021). In other words, although *Z. muelleri* may tolerate or benefit from future heatwaves, associated species, like invertebrates and fish, could be negatively affected (Smale et al., 2019). For example, the ubiquitous co-occurring habitat-forming cockle, *Austrovenus stutchburyi*, is likely to suffer from stronger and more frequent warming-induced hypoxia events (Salmond & Wing, 2022) with potentially complex impacts on the ecology of NZ seagrass meadows (Thomsen et al., 2016). These scenarios suggest that some ecosystem functions of seagrass ecosystems in NZ may still deteriorate from restructuring under warmer conditions.

Still, we did observe a few seagrass losses associated with SSTa and coincident with the 2017/18 marine heatwave, particularly in Nelson Haven, but it is possible that covarying factors could have caused this temporary loss, as the thermal tolerance of *Z. muelleri* indicate that SSTa may not be the causal driver of seagrass loss. For example, Nelson Haven is classified with 'moderate-high' vulnerability to stressors other than temperature and may have experienced declining water quality, like increasing sediment loading and eutrophication (Stevens & Robertson, 2017). Furthermore, while photosynthetic rates of *Z. muelleri* remain positive at high temperatures approaching its thermal limit, optimal light conditions are still required (Collier et al., 2011), that is, *Z. muelleri* may not benefit from warmer temperatures if water quality is poor. Indeed, historical declines in NZ seagrasses have typically been attributed to increased sedimentation, eutrophication, and possible competition from algal blooms (Siciliano et al., 2019; Thomsen et al., 2016; Turner & Schwarz, 2006; Zabarte-Maeztu et al., 2022). These studies suggest that localized human stressors may be more important direct causes of seagrass declines than warming and/or could amplify warming effects.

Co-occurring algae, limitations, and opportunities

The increased extent of seagrass in the Avon Heathcote Estuary with increasing SSTa potentially reflects a positive response to temperatures approaching *Z. muelleri*'s thermal optima. However, the green algae *Ulva* spp. co-occurs with *Z. muelleri* in this estuary (Siciliano et al., 2019; Thomsen et al., 2016, 2020) and could have contributed to increased detection of green reflectance

that contaminates the spectral response of seagrass (Ramsey III et al., 2012). However, our many field observations from the estuary indicate that *Ulva* within the analyzed spatial polygon rarely forms monospecific and independent patches but instead is found entangled around seagrass shoots (i.e., the presence of *Ulva* would thereby increase the likelihood of detecting true seagrass patches; Siciliano et al., 2019; Thomsen et al., 2016, 2020). Moreover, our satellite analyses were complemented by percentage cover data derived from close-up photographs and high-quality drone images where seagrass and *Ulva* are easy to distinguish (Figure S6) as well as published seagrass habitat maps (Table S2) which all show dominance of seagrasses compared with ephemeral *Ulva*. We also note that the estuaries where the warming predictors were significant also had relatively low algal cover (Figure S6); that is, our results are unlikely to be affected by algae. Nevertheless, the presence of co-occurring green algae highlights the importance of collecting field-based ground truth data.

Another study limitation is that pixels represented seagrass presence, not density, and that fragmentation and aggregation implied simple expansion or contraction of binary seagrass patches (detected with a cutoff related to the strength of seagrass spectral response; Cuevas et al., 2021; Lyons et al., 2012). However, future studies could instead incorporate analysis of densities by applying bio-optical algorithms to predict density from greenness (Dierssen et al., 2003; Hill et al., 2014; Lebrasse et al., 2022) or by implementing more detailed ground truthing targeting different percent cover and discretely designating them as classes for training and classification (Martin et al., 2020). Such detailed ground truthing is, however, labor-intensive, but some local managers do regularly measure percent cover of seagrass in field-based monitoring programs (e.g., Crawshaw, 2020; Stevens & Forrest, 2020). Moreover, since estuaries have different topographies, tidal flow, catchment characteristics and local anthropogenic stressors, like sedimentation, future examination of seagrass seascape metrics could analyze the influence of all these attributes, many of which can be derived from satellite imagery (Chefaoui et al., 2016). Lastly, radiometric inconsistencies in multidate Planet-Scope scenes have been reported that affect classification accuracy (Frazier & Hemingway, 2021; Wicaksono et al., 2022). However, the new Sentinel-harmonized image products used here show improved radiometric consistency across the sensor constellation as indicated by our evaluation of images from the same geographic location collected by different sensors on the same day (R. Zimmerman, unpublished). However, a rigorous evaluation of radiometric consistency of these newest products is beyond the scope of this paper. Despite these

limitations, as well as those imposed by co-occurring algae, cloud cover, limited spectral resolution, tidal elevation, and lack of control of temporal sampling scheme, our analysis still demonstrated that satellite-based methods can provide quantitative maps of seagrass meadows in turbid estuaries useful for both research and management applications. Thus, optimization and automatization of remote sensing data, including integration with artificial intelligence tools and species distribution modeling, for application in seagrass ecology would provide much improved information about the spatiotemporal dynamics of estuarine seagrasses.

Conclusions

Our analyses highlighted that intertidal and shallow subtidal seagrass meadows from turbid estuaries in NZ are dynamic in areal extent, individual patch sizes and patch configurations, across sites, seasons, and years and that SST and SST anomalies are potential drivers of many seascape changes, because seagrass extent in some estuaries was positively associated with these thermal predictors. Furthermore, the marine heatwave did not appear to drive significant seagrass loss which could be a sign of stability or resilience. However, the interaction between seagrass metrics and the tested environmental drivers is likely complicated by local conditions. Hence, we emphasize that fine-scale local water quality data would be valuable to detect which factors drive seagrass configuration. Nonetheless, despite methodological limitations, like inability to differentiate seagrass from green algae, and potentially poor detection of the sparsest seagrasses, the remote sensing workflow used here offers a powerful tool to analyze temporal changes across multiple spatiotemporal scales with lesser efforts. This study could provide a baseline for methodological optimization and to guide future monitoring of seagrasses to better detect impacts from increasing anthropogenic stressors and climate change.

Author Contributions

KJEC led the writing of the manuscript, and collected, analysed, and visualised the data. KJEC and MST conceived the ideas. MST and RCZ reviewed and edited the manuscript, provided methodological resources, and supervised research execution. All authors contributed critically to the drafts and gave final approval for publication.

Acknowledgments

References

Alfaro, A.C. (2006) Benthic macro-invertebrate community composition within a mangrove/seagrass estuary in northern New Zealand. *Estuarine, Coastal and Shelf Science*, **66**, 97–110.

Arellano-Méndez, L.U., Mora-Olivo, A., Zamora-Tovar, C., De La Rosa-Manzano, E., Torres-Castillo, J.A. & Bello-Pineda, J. (2019) Structural complexity of tropical seagrasses meadows in a temperate lagoon in the Gulf of Mexico. A landscape ecology approach. *Journal of Coastal Conservation*, **23**, 969–976.

Arias-Ortiz, A., Serrano, O., Masqué, P., Lavery, P.S., Mueller, U., Kendrick, G.A. et al. (2018) A marine heatwave drives massive losses from the world's largest seagrass carbon stocks. *Nature Climate Change*, **8**, 338–344.

Baumstark, R.D. (2018) *Remote sensing and spatial metrics for quantifying seagrass landscape changes: a study on the 2011 Indian river lagoon Florida seagrass die-off event*. PhD Thesis. University of South Florida, Tampa, FL.

Bell, S.S., Fonseca, M.S. & Stafford, N.B. (2007) Seagrass ecology: new contributions from a landscape perspective. In: Larkum, A.W.D., Orth, R.J. & Duarte, C.M. (Eds.) *Seagrasses: Biology, Ecology and Conservation*. Dordrecht: Springer Netherlands, pp. 625–645.

Bryan, K., Tay, H., Pilditch, C., Lundquist, C. & Hunt, H. (2007) The effects of seagrass (*Zostera muelleri*) on boundary-layer hydrodynamics in Whangapoua Estuary, New Zealand. *Journal of Coastal Research*, **50**, 668–672.

Bulmer, R., Kelly, S. & Jeffs, A. (2016) Light requirements of the seagrass, *Zostera muelleri*, determined by observations at the maximum depth limit in a temperate estuary, New Zealand. *New Zealand Journal of Marine and Freshwater Research*, **50**, 183–194.

Chamberlain, S. (2021) rerddap: general purpose client for 'ERDDAP' servers. R package version 0.7.6.

Chandra, M.A. & Bedi, S.S. (2021) Survey on SVM and their application in image classification. *International Journal of Information Technology*, **13**, 1–11.

Chartrand, K.M., Bryant, C.V., Carter, A.B., Ralph, P.J. & Rasheed, M.A. (2016) Light thresholds to prevent dredging impacts on the Great Barrier Reef seagrass, *Zostera muelleri* ssp. *capricorni. Frontiers in Marine Science*, **3**, 106.

Chefaoui, R.M., Assis, J., Duarte, C.M. & Serrão, E.A. (2016) Large-scale prediction of seagrass distribution integrating landscape metrics and environmental factors: the case of *Cymodocea nodosa* (Mediterranean–Atlantic). *Estuaries and Coasts*, **39**, 123–137.

Chiang, Y.-Y., Leyk, S. & Knoblock, C.A. (2014) A survey of digital map processing techniques. *ACM Computing Surveys (CSUR)*, **47**, 1–44.

Coffer, M.M., Graybill, D.D., Whitman, P.J., Schaeffer, B.A., Salls, W.B., Zimmerman, R.C. et al. (2023) Providing a framework for seagrass mapping in United States coastal ecosystems using high spatial resolution satellite imagery. *Journal of Environmental Management*, **337**, 117669.

Coffer, M.M., Schaeffer, B.A., Zimmerman, R.C., Hill, V., Li, J., Islam, K.A. et al. (2020) Performance across WorldView-2 and RapidEye for reproducible seagrass mapping. *Remote Sensing of Environment*, **250**, 112036.

Cohen, J. (1988) *Statistical power analysis for the behavioral sciences*, 2nd edition. Hillsdale, NJ: Lawrence Erlbaum Assoc.

Collier, C.J., Langlois, L., Ow, Y., Johansson, C., Giammusso, M., Adams, M.P. et al. (2018) Losing a winner: thermal stress and local pressures outweigh the positive effects of ocean acidification for tropical seagrasses. *New Phytologist*, **219**, 1005–1017.

Collier, C.J., Ow, Y.X., Langlois, L., Uthicke, S., Johansson, C.L., O'Brien, K.R. et al. (2017) Optimum temperatures for net primary productivity of three tropical seagrass species. *Frontiers in Plant Science*, **8**, 1446.

Collier, C.J., Uthicke, S. & Waycott, M. (2011) Thermal tolerance of two seagrass species at contrasting light levels: implications for future distribution in the Great Barrier Reef. *Limnology and Oceanography*, **56**, 2200–2210.

Crawshaw, J. (2020) *Seagrass health monitoring in Tauranga Harbor*. Bay of Plenty Regional Council Environmental Publication 2020/08.

Cuevas, E., Uribe-Martínez, A., Morales-Ojeda, S.M., Gómez-Ruíz, P.A., Núñez-Lara, E., Teutli-Hernández, C. et al. (2021) Spatial configuration of seagrass community attributes in a stressed coastal lagoon, southeastern Gulf of Mexico. *Regional Studies in Marine Science*, **48**, 102049.

Dierssen, H.M., Zimmerman, R.C., Leathers, R.A., Downes, T.V. & Davis, C.O. (2003) Ocean color remote sensing of seagrass and bathymetry in The Bahamas Banks by high-resolution airborne imagery. *Limnology and Oceanography*, **48**, 444–455.

Dos Santos, V.M. & Matheson, F.E. (2017) Higher seagrass cover and biomass increases sexual reproductive effort: a rare case study of *Zostera muelleri* in New Zealand. *Aquatic Botany*, **138**, 29–36.

Drucker, H., Burges, C., Kaufman, L., Smola, A. & Vapnik, V. (1996) Linear support vector regression machines. *Advances in Neural Information Processing Systems*, **9**, 155–161.

Dunic, J.C., Brown, C.J., Connolly, R.M., Turschwell, M.P. & Côté, I.M. (2021) Long-term declines and recovery of meadow area across the world's seagrass bioregions. *Global Change Biology.*, **27**, 4096–4109.

Enwright, N.M., Darnell, K.M. & Carter, G.A. (2022) Lacunarity as a tool for assessing landscape configuration over time and informing long-term monitoring: an example using seagrass. *Landscape Ecology*, **37**, 2689–2705.

Fortes, M.D. (2012) Historical review of seagrass research in The Philippines. *Coastal Marine Science*, **35**, 181–187.

Frazier, A.E. & Hemingway, B.L. (2021) A technical review of planet Smallsat data: practical considerations for processing and using PlanetScope imagery. *Remote Sensing*, **13**, 3930.

Graeme, M. (2012) *Estuarine vegetation survey - Kawhia Harbour*. Waikato Regional Council Technical Report 2014/16.

Grizzle, R.E., Short, F.T., Newell, C.R., Hoven, H. & Kindblom, L. (1996) Hydrodynamically induced synchronous waving of seagrasses: 'monami' and its possible effects on larval mussel settlement. *Journal of Experimental Marine Biology and Ecology*, **206**, 165–177.

Hammer, K.J., Borum, J., Hasler-Sheetal, H., Shields, E.C., Sand-Jensen, K. & Moore, K.A. (2018) High temperatures cause reduced growth, plant death and metabolic changes in eelgrass *Zostera marina. Marine Ecology Progress Series*, **604**, 121–132.

Helsel, D.R. & Frans, L.M. (2006) Regional Kendall test for trend. *Environmental Science & Technology*, **40**, 4066–4073.

Helsel, D.R., Hirsch, R.M., Ryberg, K.R., Archfield, S.A. & Gilroy, E.J. (2020) *Statistical methods in water resources*. Report 4-A3, Reston, VA.

Hesselbarth, M.H.K., Sciaini, M., With, K.A., Wiegand, K. & Nowosad, J. (2019) landscapemetrics: an open-source *R* tool to calculate landscape metrics. *Ecography*, **42**, 1648–1657.

Hill, V.J., Zimmerman, R.C., Bissett, W.P., Dierssen, H. & Kohler, D.D.R. (2014) Evaluating light availability, seagrass biomass, and productivity using hyperspectral airborne remote sensing in Saint Joseph's Bay, Florida. *Estuaries and Coasts*, **37**, 1467–1489.

Hirsch, R.M. & Slack, J.R. (1984) A nonparametric trend test for seasonal data with serial dependence. *Water Resources Research*, **20**, 727–732.

Howard, J., Sutton-Grier, A., Herr, D., Kleypas, J., Landis, E., McLeod, E. et al. (2017) Clarifying the role of coastal and marine systems in climate mitigation. *Frontiers in Ecology and the Environment*, **15**, 42–50.

Hume, T., Gerbeaux, P., Hart, D.E., Kettles, H. & Neale, D. (2016) *A classification of New Zealand's coastal hydrosystems*.

Hamilton: National Institute of Water & Atmospheric Research.

Hyndes, G.A., Heck, K.L., Jr., Vergés, A., Harvey, E.S., Kendrick, G.A., Lavery, P.S. et al. (2017) Accelerating tropicalization and the transformation of temperate seagrass meadows. *Bioscience*, **66**, 938–948.

Irlandi, E., Ambrose, W., Jr. & Orlando, B. (1995) Landscape ecology and the marine environment: how spatial configuration of seagrass habitat influences growth and survival of the bay scallop. *Oikos*, **72**, 307–313.

Jordà, G., Marbà, N. & Duarte, C.M. (2012) Mediterranean seagrass vulnerable to regional climate warming. *Nature Climate Change*, **2**, 821–824.

Kaufman, K.A. & Bell, S.S. (2022) The use of imagery and GIS techniques to evaluate and compare seagrass dynamics across multiple spatial and temporal scales. *Estuaries and Coasts*, **45**, 1028–1044.

Kendall, M.G. (1938) A new measure of rank correlation. *Biometrika*, **30**, 81–93.

Kohlmeier, D., Pilditch, C.A., Bornman, J.F. & Bischof, K. (2014) Site specific differences in morphometry and photophysiology in intertidal *Zostera muelleri* meadows. *Aquatic Botany*, **116**, 104–109.

Lavery, P.S., Mateo, M.-Á., Serrano, O. & Rozaimi, M. (2013) Variability in the carbon storage of seagrass habitats and its implications for global estimates of blue carbon ecosystem service. *PLoS One*, **8**, e73748.

Lebrasse, M.C., Schaeffer, B.A., Coffer, M.M., Whitman, P.J., Zimmerman, R.C., Hill, V.J. et al. (2022) Temporal stability of seagrass extent, leaf area, and carbon storage in St. Joseph Bay, Florida: a semi-automated remote sensing analysis. *Estuaries and Coasts*, **45**, 2082–2101.

Lundquist, C.J., Jones, T.C., Parkes, S.M. & Bulmer, R.H. (2018) Changes in benthic community structure and sediment characteristics after natural recolonisation of the seagrass *Zostera muelleri*. *Scientific Reports*, **8**, 1–9.

Lyons, M.B., Phinn, S.R. & Roelfsema, C.M. (2012) Long term land cover and seagrass mapping using Landsat and object-based image analysis from 1972 to 2010 in the coastal environment of South East Queensland, Australia. *ISPRS Journal of Photogrammetry and Remote Sensing*, **71**, 34–46.

Madarasz-Smith, A. & Shanahan, B. (2020) *State of the Hawke's Bay coastal marine environment: 2013 to 2018*. Napier: Hawkes Bay Regional Council Publication. No. 5425.

Mangiafico, S. (2022) rcompanion: functions to support extension education program evaluation. R package version 2.4.18.

Mann, H.B. (1945) Nonparametric tests against trend. *Econometrica: Journal of the Econometric Society*, **13**, 245–259.

Marbà, N. & Duarte, C.M. (2010) Mediterranean warming triggers seagrass (*Posidonia oceanica*) shoot mortality. *Global Change Biology*, **16**, 2366–2375.

Marchetto, A. & Marchetto, M.A. (2021) Package 'rkt'. *Technology*, **40**, 4066–4073.

Martin, R., Ellis, J., Brabyn, L. & Campbell, M. (2020) Change-mapping of estuarine intertidal seagrass (*Zostera muelleri*) using multispectral imagery flown by remotely piloted aircraft (RPA) at Wharekawa Harbour, New Zealand. *Estuarine, Coastal and Shelf Science*, **246**, 107046.

Matheson, F.E. (2018) *Seagrass assessment for Pōrangahau Estuary, Hawkes Bay*. NIWA client report 2018301HN. Prepared for Hawkes Bay Regional Council: 19.

McGarigal, K., Cushman, S.A. & Ene, E. (2012) *FRAGSTATS v4: spatial pattern analysis program for categorical and continuous maps*. Computer software program produced by the authors at the University of Massachusetts, Amherst. 15.

McGlathery, K.J., Sundbäck, K. & Anderson, I.C. (2007) Eutrophication in shallow coastal bays and lagoons: the role of plants in the coastal filter. *Marine Ecology Progress Series*, **348**, 1–18.

McKenzie, L.J., Langlois, L.A. & Roelfsema, C.M. (2022) Improving approaches to mapping seagrass within the Great Barrier Reef: from field to spaceborne earth observation. *Remote Sensing*, **14**, 2604.

Mills, V.S. & Berkenbusch, K. (2009) Seagrass (*Zostera muelleri*) patch size and spatial location influence infaunal macroinvertebrate assemblages. *Estuarine, Coastal and Shelf Science*, **81**, 123–129.

Moore, K.A. & Jarvis, J.C. (2008) Environmental factors affecting recent summertime eelgrass diebacks in the lower Chesapeake Bay: implications for long-term persistence. *Journal of Coastal Research*, **2008**, 135–147.

Moore, K.A., Shields, E.C., Parrish, D.B. & Orth, R.J. (2012) Eelgrass survival in two contrasting systems: role of turbidity and summer water temperatures. *Marine Ecology Progress Series*, **448**, 247–258.

Munir, M. & Wicaksono, P. (2019) *Support vector machine for seagrass percent cover mapping using PlanetScope image in Labuan Bajo, East Nusa Tenggara*.

Newton, A. & Mudge, S.M. (2003) Temperature and salinity regimes in a shallow, mesotidal lagoon, the ria Formosa, Portugal. *Estuarine, Coastal and Shelf Science*, **57**, 73–85.

Nguyen, H.M., Bulleri, F., Marín-Guirao, L., Pernice, M. & Procaccini, G. (2021) Photo-physiology and morphology reveal divergent warming responses in northern and southern hemisphere seagrasses. *Marine Biology*, **168**, 129.

Nguyen, H.M., Kim, M., Ralph, P.J., Marín-Guirao, L., Pernice, M. & Procaccini, G. (2020) Stress memory in seagrasses: first insight into the effects of thermal priming and the role of epigenetic modifications. *Frontiers in Plant Science*, **11**, 494.

Nguyen, H.M., Ralph, P.J., Marín-Guirao, L., Pernice, M. & Procaccini, G. (2021) Seagrasses in an era of ocean warming: a review. *Biological Reviews*, **96**, 2009–2030.

NOAA Coral Reef Watch. (2018) *SST and SST anomaly, NOAA global coral bleaching monitoring, 5km, V.3.1,*

monthly, 1985-present. NOAA/NESDIS/STAR Coral Reef Watch program.

Orth, R.J., Carruthers, T.J.B., Dennison, W.C., Duarte, C.M., Fourqurean, J.W., Heck, K.L. et al. (2006) A global crisis for seagrass ecosystems. *Bioscience*, **56**, 987–996.

Pansini, A., La Manna, G., Pinna, F., Stipcich, P. & Ceccherelli, G. (2021) Trait gradients inform predictions of seagrass meadows changes to future warming. *Scientific Reports*, **11**, 1–12.

Petrou, K., Jimenez-Denness, I., Chartrand, K., McCormack, C., Rasheed, M. & Ralph, P. (2013) Seasonal heterogeneity in the photophysiological response to air exposure in two tropical intertidal seagrass species. *Marine Ecology Progress Series*, **482**, 93–106.

Planet Team. (2018) *Planet imagery product specifications*. San Francisco, CA: Planet Team.

Planet Team. (2022) *Planet imagery product specifications*. San Francisco, CA: Planet Team.

R Core Team. (2021) *R: a language and environment for statistical computing*. Vienna, Austria: R Foundation for Statistical Computing.

Ramage, D.L. & Schiel, D.R. (1999) Patch dynamics and response to disturbance of the seagrass *Zostera novazelandica* on intertidal platforms in southern New Zealand. *Marine Ecology Progress Series*, **189**, 275–288.

Ramsey, E., III, Rangoonwala, A., Thomsen, M.S. & Schwarzschild, A. (2012) Spectral definition of the macro-algae *Ulva curvata* in the back-barrier bays of the Eastern Shore of Virginia, USA. *International Journal of Remote Sensing*, **33**, 586–603.

Robertson, B.M., Stevens, L., Robertson, B., Zeldis, J., Green, M., Madarasz-Smith, A. et al. (2016) *NZ Estuary Trophic Index Screening Tool 1. Determining eutrophication susceptibility using physical and nutrient load data*. Prepared for Envirolink Tools Project: Estuarine Trophic Index, MBIE/NIWA Contract No: C01X1420. 47 p.

Robertson, B.P. & Savage, C. (2021) Thresholds in catchment nitrogen load for shifts from seagrass to nuisance macroalgae in shallow intertidal estuaries. *Limnology and Oceanography*, **66**, 1353–1366.

RStudio Team. (2021) *RStudio: integrated development environment for R*. Boston, MA: RStudio PBC.

Salinger, M.J., Diamond, H.J., Behrens, E., Fernandez, D., Fitzharris, B.B., Herold, N. et al. (2020) Unparalleled coupled ocean-atmosphere summer heatwaves in the New Zealand region: drivers, mechanisms and impacts. *Climatic Change*, **162**, 485–506.

Salmond, N.H. & Wing, S.R. (2022) Sub-lethal and lethal effects of chronic ammonia exposure and hypoxia on a New Zealand bivalve. *Journal of Experimental Marine Biology and Ecology*, **549**, 151696.

Schwarz, A.M. (2004) Contribution of photosynthetic gains during tidal emersion to production of *Zostera capricorni* in a North Island, New Zealand estuary. *New Zealand Journal of Marine and Freshwater Research*, **38**, 809–818.

Siciliano, A., Schiel, D.R. & Thomsen, M.S. (2019) Effects of local anthropogenic stressors on a habitat cascade in an estuarine seagrass system. *Marine and Freshwater Research*, **70**, 1129–1142.

Sims, R.P., Bedington, M., Schuster, U., Watson, A.J., Kitidis, V., Torres, R. et al. (2022) Tidal mixing of estuarine and coastal waters in the western English Channel is a control on spatial and temporal variability in seawater CO_2. *Biogeosciences*, **19**, 1657–1674.

Smale, D.A., Wernberg, T., Oliver, E.C.J., Thomsen, M., Harvey, B.P., Straub, S.C. et al. (2019) Marine heatwaves threaten global biodiversity and the provision of ecosystem services. *Nature Climate Change*, **9**, 306–312.

Stevens, L. & Forrest, B. (2020) *Macroalgal monitoring of new river estuary*. Salt Ecology Report 054, prepared for Environment Southland.

Stevens, L.M. & Robertson, B.P. (2017) *Nelson region estuaries: vulnerability assessment and monitoring recommendations*. Nelson: Wriggle Coastal Management for Nelson City Council.

Strydom, S., Murray, K., Wilson, S., Huntley, B., Rule, M., Heithaus, M. et al. (2020) Too hot to handle: unprecedented seagrass death driven by marine heatwave in a World Heritage Area. *Global Change Biology*, **26**, 3525–3538.

Sully, S. & van Woesik, R. (2020) Turbid reefs moderate coral bleaching under climate-related temperature stress. *Global Change Biology*, **26**, 1367–1373.

Tait, L.W., Thoral, F., Pinkerton, M.H., Thomsen, M.S. & Schiel, D.R. (2021) Loss of Giant Kelp, *Macrocystis pyrifera*, driven by marine heatwaves and exacerbated by poor water clarity in New Zealand. *Frontiers in Marine Science*, **8**, 721087.

Thomsen, M.S., Hildebrand, T., South, P.M., Foster, T., Siciliano, A., Oldach, E. et al. (2016) A sixth-level habitat cascade increases biodiversity in an intertidal estuary. *Ecology and Evolution*, **6**, 8291–8303.

Thomsen, M.S., Mondardini, L., Alestra, T., Gerrity, S., Tait, L., South, P.M. et al. (2019) Local extinction of bull kelp (*Durvillaea* spp.) due to a marine heatwave. *Frontiers in Marine Science*, **6**, 84.

Thomsen, M.S., Mondardini, L., Thoral, F., Gerber, D., Montie, S., South, P.M. et al. (2021) Cascading impacts of earthquakes and extreme heatwaves have destroyed populations of an iconic marine foundation species. *Diversity and Distributions*, **27**, 2369–2383.

Thomsen, M.S., Moser, A., Pullen, M., Gerber, D. & Flanagan, S. (2020) Seagrass beds provide habitat for crabs, shrimps and fish in two estuaries on the South Island of New Zealand. *bioRxiv*. Report to Environment Canterbury: 55.

Thomsen, M.S. & South, P. (2019) Communities and attachment networks associated with primary, secondary and alternative foundation species; a case study of stressed and disturbed stands of southern bull kelp. *Diversity*, **11**, 56.

Thomson, J.A., Burkholder, D.A., Heithaus, M.R., Fourqurean, J.W., Fraser, M.W., Statton, J. et al. (2015) Extreme

temperatures, foundation species, and abrupt ecosystem change: an example from an iconic seagrass ecosystem. *Global Change Biology*, **21**, 1463–1474.

Traganos, D., Aggarwal, B., Poursanidis, D., Topouzelis, K., Chrysoulakis, N. & Reinartz, P. (2018) Towards global-scale seagrass mapping and monitoring using Sentinel-2 on Google earth engine: the case study of the Aegean and Ionian seas. *Remote Sensing*, **10**, 1227.

Traganos, D. & Reinartz, P. (2018) Machine learning-based retrieval of benthic reflectance and *Posidonia oceanica* seagrass extent using a semi-analytical inversion of Sentinel-2 satellite data. *International Journal of Remote Sensing*, **39**, 9428–9452.

Tukey, J.W. (1977) *Exploratory data analysis*. Reading, MA: Addison-Wesley.

Turner, S., Hewitt, J., Wilkinson, M., Morrisey, D., Thrush, S., Cummings, V. et al. (1999) Seagrass patches and landscapes: the influence of wind-wave dynamics and hierarchical arrangements of spatial structure on macrofaunal seagrass communities. *Estuaries*, **22**, 1016–1032.

Turner, S. & Schwarz, A.-M. (2006) Management and conservation of seagrass in New Zealand: an introduction. *Science for Conservation*, **264**, 1–90.

Tuya, F., Hernandez-Zerpa, H., Espino, F. & Haroun, R. (2013) Drastic decadal decline of the seagrass *Cymodocea nodosa* at Gran Canaria (eastern Atlantic): interactions with the green algae *Caulerpa prolifera*. *Aquatic Botany*, **105**, 1–6.

Uhrin, A.V. & Turner, M.G. (2018) Physical drivers of seagrass spatial configuration: the role of thresholds. *Landscape Ecology*, **33**, 2253–2272.

Unsworth, R.K., De Grave, S., Jompa, J., Smith, D.J. & Bell, J.J. (2007) Faunal relationships with seagrass habitat structure: a case study using shrimp from the Indo-Pacific. *Marine and Freshwater Research*, **58**, 1008–1018.

Veettil, B.K., Ward, R.D., Lima, M.D.A.C., Stankovic, M., Hoai, P.N. & Quang, N.X. (2020) Opportunities for seagrass research derived from remote sensing: a review of current methods. *Ecological Indicators*, **117**, 106560.

Wicaksono, P., Maishella, A., Lazuardi, W. & Muhammad, F.H. (2022) Consistency assessment of multi-date PlanetScope imagery for seagrass percent cover mapping in different seagrass meadows. *Geocarto International*, **37**, 15161–15186.

Widya, L.K., Kim, C.-H., Do, J.-D., Park, S.-J., Kim, B.-C. & Lee, C.-W. (2023) Comparison of satellite imagery for identifying seagrass distribution using a machine learning algorithm on the eastern coast of South Korea. *Journal of Marine Science and Engineering*, **11**, 701.

Yarnall, A.H., Byers, J.E., Yeager, L.A. & Fodrie, F.J. (2022) Comparing edge and fragmentation effects within seagrass communities: a meta-analysis. *Ecology*, **103**, e3603.

York, P.H., Gruber, R.K., Hill, R., Ralph, P.J., Booth, D.J. & Macreadie, P.I. (2013) Physiological and morphological responses of the temperate seagrass *Zostera muelleri* to

multiple stressors: investigating the interactive effects of light and temperature. *PLoS One*, **8**, e76377.

Zabarte-Maeztu, I., D'Archino, R., Matheson, F.E., Manley-Harris, M. & Hawes, I. (2022) First record of *Chaetomorpha ligustica* (Cladophoraceae, Cladophorales) smothering the seagrass *Zostera muelleri* in a New Zealand estuary. *New Zealand Journal of Marine and Freshwater Research*, **2022**, 1–12.

Zabarte-Maeztu, I., Matheson, F.E., Manley-Harris, M., Davies-Colley, R.J., Oliver, M. & Hawes, I. (2020) Effects of fine sediment on seagrass meadows: a case study of *Zostera muelleri* in Pāuatahanui inlet, New Zealand. *Journal of Marine Science and Engineering*, **8**, 645.

Zeldis, J., Plew, D., Whitehead, A., Madarasz-Smith, A., Oliver, M., Stevens, L. et al. (2017) *The New Zealand Estuary Trophic Index (ETI) tools: web tool 1 - determining eutrophication susceptibility using physical and nutrient load data*. Ministry of Business, Innovation and Employment Envirolink Tools: C01X1420.

Supporting Information

Additional supporting information may be found online in the Supporting Information section at the end of the article.

Table S1. Summary of class-level landscape metrics analysed in this study adapted from McGarigal et al. (2012) and Hesselbarth et al. (2019).

Table S2. References used either as sole reference or as complement to photos and drone images.

Table S3. Summary of inter-annual mean percent change of seagrass area (in ha) from winter to summer in each estuary (rows highlighted in blue denotes positive change, red denotes negative change).

Figure S1. Seagrass areal extent (transformed) as a function of tidal height during image acquisition time in each site.

Figure S2. Summary of Multiple Linear Regression Tests (slopes) of landscape metrics versus monthly K_d-490.

Figure S3. Summary of Multiple Linear Regression Tests (slopes) of landscape metrics versus monthly Chl-*a* concentration.

Figure S4. Pixel location of satellite-derived monthly data of covariates such as SST, SST anomaly, K_d-490 (proxy for turbidity), and Chl-*a* (proxy for nutrients).

Figure S5. Area of Interests (AOIs) in this study excluding land.

Figure S6. Average percent cover data of seagrass and green algae analysed from (a) photo images in 2016 and (b, c) photo and drone images in 2020 from the same estuaries in South Island that we used for satellite imagery analysis.